INTERNATIONAL JOURNAL FOR NUMERICAL METHODS IN FLUIDS, VOL. 18, 1061–1071 (1994)

APPLICATION OF STREAMWISE DIFFUSION TO TIME-DEPENDENT FREE CONVECTION OF LIQUID METALS

MATTHEW A. McCLELLAND

Lawrence Livermore National Laboratory, Livermore, CA 94550, U.S.A.

SUMMARY

A numerical analysis is given for the application of streamwise diffusion to high-intensity flows with marginal spatial resolution. Terms are added to the momentum equation which are similar to those used in the Petrov–Galerkin, Taylor–Galerkin and balancing tensor diffusivity methods. Values for the streamwise viscosity are obtained from mesh refinement studies. An illustration is given for the time-dependent free convection of a liquid metal in a cavity with differentially heated sided walls. The spatial problem is solved with the Galerkin finite element method and the time integration is performed with the backward Euler method. Solution quality and computation time are compared for results with and without added streamwise diffusion. For the cases presented, streamwise diffusion eliminates spurious oscillations and saves computation time without compromising the solution.

KEY WORDS Streamwise diffusion Taylor–Galerkin method Finite element method Free convection Liquid metals

1. INTRODUCTION

Transition flows between steady state laminar and turbulent are of interest in a wide variety of applications. One large class includes liquid metal flows in crystal growth, welding, casting and electron beam vaporization systems. High flow intensities results from strong buoyancy and surface tension forces and small metal viscosities. Often high spatial resolution is needed to obtain accurate solutions. If mass diffusion is included in the flow model, even greater resolution is required, since diffusivities for mass are smaller than for momentum. In either case this resolution can require excessive amounts of computing time for many two-dimensional and most three-dimensional problems. In the case of marginal or inadequate spatial resolution, spurious oscillations appear which may be expensive to track using time integration methods with error control.

A number of investigators have addressed this problem by increasing the diffusive component in the direction of flow where it is needed most. In the direction normal to flow the diffuse component is left unchanged. Brooks and Hughes[1] developed a streamline upwind/Petrov–Galerkin formulation for flows dominated by convection. Weighting functions for the streamline diffusion terms depend on the mesh, time step and flow field. The method was successfully applied to a vortex-shedding problem at a moderate Reynolds number. Streamwise diffusion terms of similar form also appear in the development of Taylor–Galerkin methods for transient flows dominated by convection.[2,3] It was found that these terms could also be of help in the elimination of spurious oscillations in steady state flows. In this case the theoretical base is

This paper was prepared under the auspices of the U.S. Government and is therefore in the public domain.

Received 7 April 1992
Revised 25 October 1993

weaker and the use and weighting of the terms are largely empirical. Gresho *et al.*[4] employed these terms in balancing the negative tensor diffusivity generated by the forward Euler method. They also note the merits of applying this approach in an *ad hoc* fashion to steady state problems.

In this paper we employ streamwise diffusion terms of the same form, utilizing an empirical method to determine the coefficients. Mesh refinement studies are performed to determine the maximum convective component that can be resolved by a given mesh. For higher flow intensities streamwise diffusion is added so that the convective component does not exceed the maximum value. Application is given to the free convection system of Figure 1 which has been considered by a number of investigators.[5–9] Temperature-induced buoyancy forces drive flow in a shallow two-dimensional cavity with vertical walls maintained at different temperatures. We employ the Galerkin finite element and backward Euler methods to obtain solutions at flow intensities as high as those encountered in electron beam vaporizers. Solution accuracy and computing time are compared for reference solutions and coarse mesh results with and without streamwise diffusion.

2. BASIC EQUATIONS

Consider a Newtonian liquid with constant physical properties, except the density which varies linearly with temperature according to the Boussinesq approximation. The non-dimensional mass, momentum and energy equations are

$$\nabla \cdot \mathbf{v} = 0, \tag{1}$$

$$\sqrt{(Gr)}\left(\frac{\partial \mathbf{v}}{\partial t} + \mathbf{v} \cdot \nabla \mathbf{v}\right) = -\nabla \cdot \boldsymbol{\pi} + \left(\frac{1}{St} - \sqrt{GrT}\right)\boldsymbol{\delta}_g, \tag{2}$$

$$\sqrt{(Gr)}Pr\left(\frac{\partial T}{\partial t} + \mathbf{v} \cdot \nabla T\right) = -\nabla \cdot \mathbf{q}. \tag{3}$$

The dimensionless total stress tensor π and heat flux vector $\mathbf{q}$ are given by

$$\boldsymbol{\pi} = p\boldsymbol{\delta} - [\nabla \mathbf{v} + (\nabla \mathbf{v})^{\dagger}], \tag{4}$$

$$\mathbf{q} = -\nabla T. \tag{5}$$

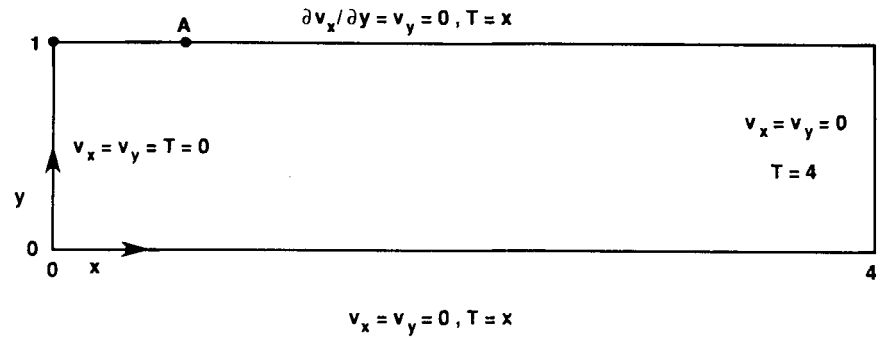

Figure 1. Co-ordinates and boundary conditions for natural convection in a rectangular cavity. Point A is located at $x = 0{\cdot}8$, $y = 1$

With 'pluses' denoting dimensional variables, the scaled variables are

$$t = t^+ v_s/h, \qquad \mathbf{x} = \mathbf{x}^+/h, \qquad \mathbf{v} = \mathbf{v}^+/v_s,$$
$$\boldsymbol{\pi} = \boldsymbol{\pi}^+ h/\mu v_s, \qquad p = p^+ h/\mu v_s, \tag{6}$$
$$T = (T^+ - T_0)L/h(T_0 - T_1), \qquad \mathbf{q} = \mathbf{q}^+ L/k(T_1 - T_0).$$

Here h and L are the height and length of the trough respectively. Also, T_0 and T_1 are the dimensional temperatures at the boundaries $x = 0$ and $x = 4$ respectively. The properties μ and k are the viscosity and thermal conductivity evaluated at T_0 respectively. A velocity standard is obtained from a characteristic balance of buoyancy and inertial forces:

$$v_s = [\beta(T_1 - T_0)gh^2/L]^{1/2}. \tag{7}$$

Here β is the volumetric thermal expansion coefficient. The dimensionless groups are

$$Gr = \beta(T_1 - T_0)gh^4/v^2L, \qquad Pr = v/\alpha, \qquad St = [\beta(T_1 - T_0)v^2/gh^2L]^{1/2}, \tag{8}$$

in which v and α are the kinematic viscosity and thermal diffusivity evaluated at T_0 respectively. Note that the Reynolds, Peclet and Rayleigh numbers are related to the Grashof and Prandtl numbers by $Re = Gr^{1/2}$, $Pe = Gr^{1/2}Pr$ and $Ra = GrPr$ respectively.

The problem statement given by equations (1)–(3) is complete with the specification of initial and boundary conditions (see Figure 1). The initial condition for a time-dependent case is a steady state solution at a lower Grashof number. The momentum boundary conditions are a shear-free condition at the boundary $y = 1$ and no-slip conditions at all other boundaries. The temperature is maintained at different values at the two vertical boundaries and linearly interpolated values are used at the other two boundaries.

3. NUMERICAL METHOD

3.1. Streamwise diffusion

At the high flow intensities of interest the effects of convection are quite important and high spatial resolution is needed to obtain accurate solutions. Unfortunately, this resolution currently requires excessive amounts of computing time for many 2D problems and most 3D problems of interest. Lower resolution leads to spurious oscillations which can be expensive to track in time. In order to reduce these oscillations, we add streamwise diffusion terms to the momentum equation (2) and the energy equation (3). The stress tensor (4) and heat flux vector (5) become

$$\boldsymbol{\pi} = p\boldsymbol{\delta} - \{(\boldsymbol{\delta} + \gamma_v \mathbf{vv}) \cdot \nabla \mathbf{v} + [(\boldsymbol{\delta} + \gamma_v \mathbf{vv}) \cdot \nabla \mathbf{v}]^\dagger\}, \tag{9}$$

$$\mathbf{q} = -(\boldsymbol{\delta} + \gamma_\alpha \mathbf{vv}) \cdot \nabla T. \tag{10}$$

It is seen that these expressions include isotropic terms corresponding to physical diffusion and added anisotropic terms with coefficients γ_v and γ_α. For $\gamma_v = \gamma_\alpha = 0$ equations (9) and (10) reduce to equations (4) and (5). By writing equations (9) and (10) in terms of velocity components tangent and normal to the direction of flow, it can be shown that the added diffusion terms are anisotropic in the direction of flow.[4] Thus diffusion is added in the streamwise direction where it is needed most.

It is convenient to characterize the added diffusion for the momentum and energy equations in terms of streamwise Grashof and Peclet numbers:

$$Gr_{sw} = Gr/(1 + \gamma_v)^2, \qquad Pe_{sw} = Pe/(1 + \gamma_\alpha). \tag{11}$$

In practice, some experimentation is required to find values of Gr_{sw} and Pe_{SW} that reduce spurious oscillations without excessive damping of the solution. For liquid metals with small values of Pr the effects of convection are much more important for momentum than energy and it is frequently useful to make the choice of $\gamma_\alpha = 0$. The following empirical procedure can then be tested to obtain a value for Gr_{sw}. Time-dependent calculations are performed for several values of Gr and no streamwise diffusion ($\gamma_v = 0$). Mesh refinement is used to establish the presence of spurious oscillations. For a given mesh there will be a maximum value Gr_{max}, above which spurious oscillations are unacceptably large. To eliminate these oscillations at higher values of Gr, we select $Gr_{sw} = Gr_{max}$. To assess accuracy, the results with streamwise diffusion should occasionally be compared with fine mesh results in which streamwise diffusion is absent. This procedure is illustrated below in Section 4.

It is useful to consider earlier applications of streamwise diffusion terms similar to those in equations (9) and (10). Donea and co-workers[2,3] developed Taylor–Galerkin methods to provide for the accurate time integration of the thermal convection–diffusion equation for cases with large convective components. One of these methods, referred to as the 'splitting-up' method, introduces streamwise diffusion under steady state conditions. For steady flows separate Taylor series expansions are obtained for the convection and diffusion terms in the expression

$$Pe\left(\frac{\partial T}{\partial t} + \mathbf{v}\cdot\nabla T\right) = \nabla^2 T \tag{12}$$

which is equation (3) with $Pe = Gr^{1/2}Pr$ (see Appendix I). These expansions are combined to give a result which includes terms of order ($Pe\Delta t^{-1}$, $Pe\Delta t^0$, $Pe\Delta t^1$, ...) and (Δt^0, Δt^1, Δt^2, ...) with $\Delta t = t_{n+1} - t_n$. For large Pe we keep terms of order $Pe\Delta t^1$ and Δt^0 since they are the most important. The resulting Taylor–Galerkin expression for the convection–diffusion equation is

$$Pe\left(\frac{T_{n+1} - T_n}{\Delta t} + \mathbf{v}\cdot\nabla T_n\right) = \nabla^2 T_n + \frac{Pe\Delta t}{2}\nabla\cdot(\mathbf{v}\mathbf{v}\cdot\nabla T_n) + \frac{\Delta t}{2}\nabla^2\left(\frac{T_{n+1} - T_n}{\Delta t}\right). \tag{13}$$

Steady state conditions are applied and the resulting expression is written in the form

$$Pe(\mathbf{v}\cdot\nabla T) = \nabla\cdot\left[\left(\boldsymbol{\delta} + \frac{Pe\Delta t}{2}\mathbf{v}\mathbf{v}\right)\cdot\nabla T\right]. \tag{14}$$

This is the steady state convection–diffusion equation plus a Taylor–Galerkin term which introduces streamwise diffusion. The theoretical base for this term is questionable, since terms with Δt should vanish under steady state conditions. Nonetheless, it is still useful. Donea *et al.*[3] employed this term in a test problem for which convective components were large and spatial resolution was inadequate. Spurious oscillations were eliminated without compromising the solution. We use this same term in equation (10) with the coefficient $Pe\Delta t/2$ replaced by γ_α. A similar approach leads to the momentum diffusion term in equation (9).

Brooks and Hughes[1] and Gresho *et al.*[4] arrived at results similar to equation (9) in their investigations of the Petrov–Galerkin method and the method of balancing tensor diffusivity respectively. The coefficient for the latter method includes Δt, similar to the Taylor–Galerkin method. However, the coefficient for the Petrov–Galerkin method is a more complex function

of the mesh, time step and flow field. These coefficients and weighting functions are applicable when specific time integration methods are employed. However, the use of streamwise diffusion terms can be much more general. They can be applied to both steady state and transient problems with a wide variety of numerical methods. If theoretical expressions are available, they can be used to select coefficients and weighting functions. Otherwise the mesh refinement approach of this paper can be employed.

3.2. Spatial discretization and time integration

The equations of change (1)–(3) are discretized in space using a mixed finite element basis set and Galerkin method.[10] On quadrilateral elements the velocity and temperature are expanded in terms of nine-node Lagrangian biquadratic polynomials and the pressure is expanded in terms of four-node bilinear polynomials. The residual expressions are formed for the equations of change (1)–(3) and the momentum and energy equations are written in the weak form. In this transformation the stress and heat flux terms are integrated by parts and $\boldsymbol{\pi}$ and $\mathbf{q}$ in the surface integrals are replaced by equations (9) and (10). The physical boundary terms are specified using the conditions shown in Figure 1. The streamwise boundary terms vanish, since streamlines do not pass through boundaries. In the more general case of inflow and outflow boundaries these terms also vanish in the absence of momentum or energy fluxes across boundaries.

Three meshes are used which are symmetric about the lines $x = 2$ and $y = 0{\cdot}5$ (see Figure 2). Element boundary locations for the quadrant ($0 \leq x \leq 2, 0 \leq y \leq 0{\cdot}5$) are given by

$$\begin{aligned} x_i &= 2[1 - \exp(2ai/n_{e,x})]/[1 - \exp(a)], \quad i = 1, 2, \ldots, n_{e,x}/2, \\ y_i &= \tfrac{1}{2}[1 - \exp(2ai/n_{e,y})]/[1 - \exp(a)], \quad i = 1, 2, \ldots, n_{e,y}/2, \end{aligned} \tag{15}$$

in which $n_{e,x}$ and $n_{e,y}$ are the numbers of elements in the x- and y-directions respectively. The parameter a is used to stretch the mesh. In the limit $a \to 0$ the spacing of nodes is uniform in each co-ordinated direction. In this study we use $a = 1{\cdot}5$ for the 48×18 mesh and $a = 1$ for the others. Finer discretizations are applied near the boundaries of the cavity to resolve boundary layers in velocity and temperature.

The discretized equations are integrated in time using the backward Euler method with automatic error control.[10,11] A predictor–corrector method is used in which a calculated error e is kept close to a prescribed error ε. For the calculations presented below, we use $\varepsilon = 1 \times 10^{-3}$ in all cases.

The non-linear algebraic equations are solved for $\mathbf{v}$, p and T using the Newton–Raphson

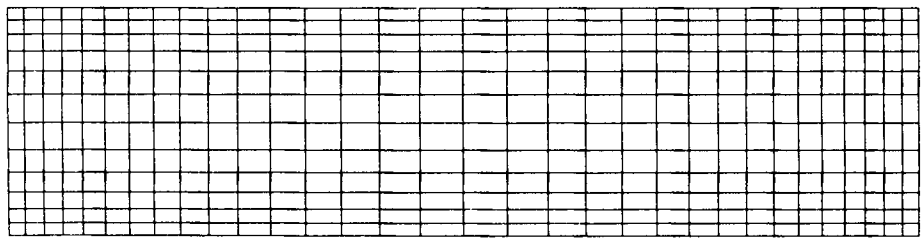

Figure 2. 32×12 finite element mesh for natural convection in a rectangular cavity; 5304 unknowns with $a = 1{\cdot}0$. Element locations are given by equations (15). Meshes not shown: 48×18 mesh, 11,698 unknowns with $a = 1{\cdot}5$; 64×24 mesh, 20,588 unknowns with $a = 1$

method, which linearizes the equations. This method is applied to all terms except the streamwise diffusion terms in equations (9) and (10). In steady state calculations these tensors are evaluated at the solution for the previous iteration as in a successive substitution method, while for time-dependent calculations they are evaluated at the predicted solution. The linear equation set is solved by Gaussian elimination using a modified frontal solver based on the one given by Hood.[12]

Using this formulation, streamwise diffusion terms can be added to an existing two- or three-dimensional finite element computer code with relatively little effort. Since equations (9) and (10) are not specific to the finite element method, application is readily made to finite difference, finite volume and other methods.

4. RESULTS

The application of streamwise diffusion is illustrated for the natural convection system of Figure 1. We use Grashof numbers of 1×10^6 and 1×10^7 which overlap the range $1 \times 10^6 \times Gr \leq 1 \times 10^8$ for electron beam vaporization of metals. In this work we use $Pr = 0{\cdot}015$ which is representative for many liquid metal systems and is a value used in previous investigations.[5–9] For the transport of energy we do not introduce streamwise diffusion in any of the calculations, since the effects of thermal convection are moderate with $Pe \leq 47{\cdot}4$. However, for $Gr = 1 \times 10^7$ streamwise diffusion is applied for the transport of momentum, since convective components are large ($Re = 3162$). In the following cases a mesh refinement study is performed at $Gr = 1 \times 10^6$ to determine the coarsest mesh for which spurious oscillations are acceptable. This mesh is then employed at 1×10^7 with and without streamwise diffusion. These results are then compared with a fine mesh solution.

For the time-dependent calculations at $Gr = 1 \times 10^6$ we use the steady state solution at $Gr = 2 \times 10^4$ as an initial condition. Contours for the streamfunction and temperature are shown in Figure 3 for the three meshes. The smooth contours for the 64 × 24 mesh suggest that the flow field is well resolved and that streamwise diffusion is not needed. The flow is quite complex with at least four cells present at any time. Some spurious oscillations are present for the 32 × 12 mesh but are essentially absent for the 48 × 18 mesh. It also appears that the timing of flow events is slightly different for the three meshes.

The velocity component v_x at location A (see Figure 1) is plotted versus time in Figure 4. As

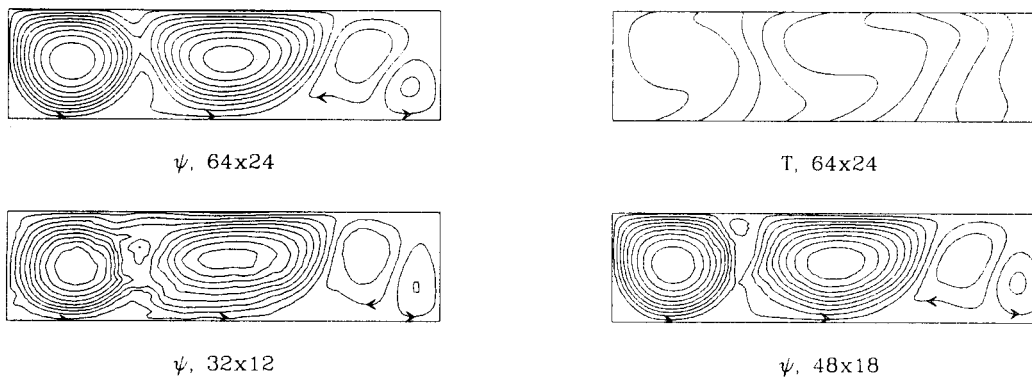

Figure 3. Streamlines and temperature contours for $Gr = 1 \times 10^6$ at $t = 7{\cdot}0$

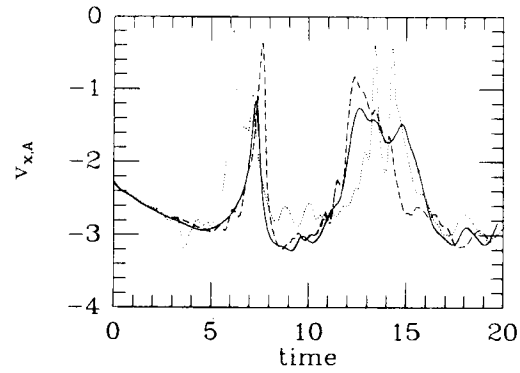

Figure 4. Time step size and v_x at location A for $Gr = 1 \times 10^6$: ———, 64 × 24; — — —, 48 × 18; ·····, 32 × 12

the mesh is refined, many of the higher-frequency fluctuations in $v_{x,A}$ are reduced or eliminated. The profiles for $v_{x,A}$ appear to be converging with mesh refinement, but there are still differences between the results for the 48 × 18 and 64 × 24 meshes. Based on these results, the spurious oscillations are judged to be acceptable for the 64 × 24 and 48 × 18 meshes but not for the 32 × 12 mesh.

Time-dependent calculations were performed for $Gr = 1 \times 10^7$ using the steady state solution at $Gr = 1 \times 10^4$ as an initial condition. Simulations were performed without streamwise diffusion for the 48 × 18 and 64 × 24 meshes and with diffusion for the 48 × 18 mesh. In the latter case we selected $Gr_{sw} = 1 \times 10^6$, since spurious oscillations are acceptable small for the case with $Gr = 1 \times 10^6$, the 48 × 18 mesh and no added streamwise diffusion (see Figures 3 and 4).

Streamlines are plotted at $t = 7{\cdot}0$ for the three cases (see Figure 5). For the 64 × 24 mesh the smooth contours indicate that the flow field is adequately resolved. For the 48 × 18 mesh the addition of streamwise diffusion eliminates spurious oscillations without altering the key features of the solution. However, the added diffusion reduces flow variations in the streamwise direction. Streamlines are unnaturally 'straightened' as is somewhat evident in the two primary cells of Figure 5. Thus streamwise diffusion must be added judiciously. Temperature contours are also

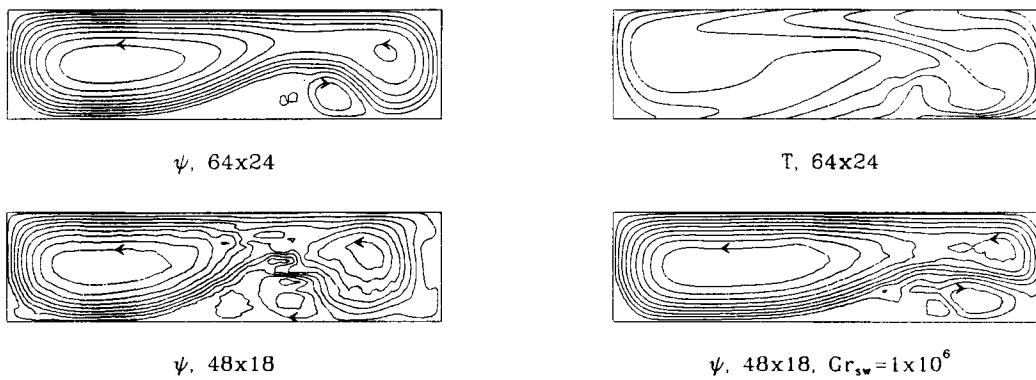

Figure 5. Streamlines and temperature contours for $Gr = 1 \times 10^7$ at $t = 7{\cdot}0$. Streamwise viscosity is added if a value of Gr_{sw} is given

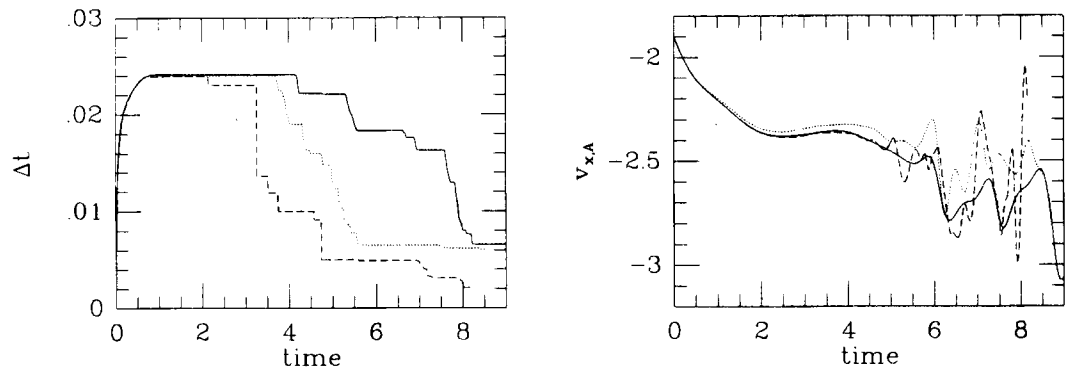

Figure 6. Time step size and v_x at location A for $Gr = 1 \times 10^7$: ———, 64 × 24; — — —, 48 × 18; ·····, 48 × 18, $Gr_{sw} = 1 \times 10^6$. Streamwise diffusion is added if a value of Gr_{sw} is given

Table I. CPU time for cases with $Gr = 1 \times 10^7$

Mesh	Gr_{sw}	Number of time steps	Total CPU time* (h)
48 × 18	1×10^7	1059	343
48 × 18	1×10^6	677	219
64 × 24	1×10^7	399	353

* CPU time on a DECstation 3100 required to reach $t = 8{\cdot}0$.

shown in Figure 5 for the 64 × 24 mesh. The curved contours reveal moderate thermal convection which is well resolved by all the meshes.

The time step size is plotted versus time in Figure 6 for the three cases. Values of Δt first increase and then decrease as the flow accelerates and increases in intensity. For $t > 2$ values of Δt are largest for the fine 64 × 24 mesh, followed by the 48 × 18 mesh with $Gr_{sw} = 1 \times 10^6$. For the 48 × 18 mesh and no added diffusion the values of Δt are significantly smaller. The smaller steps are needed to track the spurious oscillations resulting from inadequate spatial resolution.

Evolutionary plots for $v_{x,A}$ are shown in Figure 6. The results of all three cases are similar for the period $0 \leq t \leq 5$ in which the flow accelerates. As the flow intensity increases for $t \geq 5$, differences in the solutions are much more significant. Comparison between the results for the 48 × 18 and 64 × 24 meshes shows that spurious oscillations are present for the coarser mesh. With the introduction of streamwise diffusion ($Gr_{sw} = 1 \times 10^6$) these spurious oscillations are reduced in magnitude and frequency without harming the solution. For the 48 × 18 mesh there is a 36% saving in computation time, since fewer steps are required to track the solution (see Table I). In addition, the solution with streamwise diffusion requires 38% less computing time than the fine mesh solution.

5. CONCLUSIONS

The key result is the application of streamwise diffusion to a liquid metal flow with high intensity. The method is generally applicable to time-dependent transport systems with strong convective

components. Terms are added to the convection–diffusion equations which are in many respects similar to those in the Taylor–Galerkin, Petrov–Galerkin and balancing tensor diffusivity approaches. These streamwise diffusion terms are simple in form and readily implemented. The maximum resolvable convective component is determined from mesh refinement studies and coefficients for the streamwise diffusion terms are specified using scaling relationships.

Application is made to a transient liquid metal flow in a shallow cavity with differentially heated side walls. A mesh refinement study yields a maximum tolerable Grashof number of 1×10^6 for an 18×48 mesh. For the same mesh with $Gr = 1 \times 10^7$ streamwise viscosity is added to keep the streamwise Grashof number at 1×10^6. Comparison with a reference solution and results without streamwise viscosity reveals that spurious oscillations are reduced without compromising the solution. In addition, there is a significant saving in computation time.

ACKNOWLEDGEMENTS

The author expresses his appreciation to Professor Bruce A. Finlayson for helpful discussions and for providing the initial version of the finite element code. The assistance of Pamela J. Meyer in performing the simulations and Kenneth W. Westerberg in reviewing the manuscript is also gratefully acknowledged. This work was performed under the auspices of the U.S. Department of Energy by Lawrence Livermore National Laboratory under Contract W-7405-Eng-48.

APPENDIX I: THE SPLITTING-UP TAYLOR–GALERKIN (TG) METHOD

Donea *et al.*[3] developed the splitting-up TG method to provide streamwise diffusion under steady state conditions. Consider the advection–diffusion equation (12) for steady flow. Separate TG expressions are developed for the advection and diffusion terms using the Taylor series

$$T_{n+1} = T_n + \Delta t \left.\frac{\partial T}{\partial t}\right|_n + \frac{\Delta t^2}{2} \left.\frac{\partial^2 T}{\partial t^2}\right|_n + O(\Delta t^3). \tag{16}$$

The TG advection expression is obtained from

$$\frac{\partial T^a}{\partial t} = -\mathbf{v} \cdot \nabla T^a, \tag{17}$$

in which T^a denotes a solution to this expression. For an incompressible liquid

$$\mathbf{v} \cdot \nabla T = \nabla \cdot (\mathbf{v} T). \tag{18}$$

Insertion of this expression into equation (17) and a second differentiation with respect to time gives

$$\frac{\partial^2 T^a}{\partial t^2} = -\nabla \cdot \left(\mathbf{v} \frac{\partial T^a}{\partial t} \right). \tag{19}$$

Equations (17) and (19) are inserted into equation (16), keeping terms of $O(\Delta t^2)$. The resulting TG expression for the advection equation (17) is

$$\frac{T^a_{n+1} - T^a_n}{\Delta t} + \mathbf{v} \cdot \nabla T^a_n = \frac{\Delta t}{2} \nabla \cdot (\mathbf{v}\mathbf{v} \cdot \nabla T^a_n). \tag{20}$$

The TG diffusion expression is developed from

$$\frac{\partial T^{\mathrm{d}}}{\partial t} = \frac{1}{Pe} \nabla^2 T^{\mathrm{d}}. \tag{21}$$

This expression and its time derivative are inserted into equation (16) to give

$$Pe\left(\frac{T^{\mathrm{d}}_{n+1} - T^{\mathrm{d}}_{n}}{\Delta t}\right) = \nabla^2 T^{\mathrm{d}}_{n} + \frac{\Delta t}{2} \nabla^2 \left(\frac{\partial T^{\mathrm{d}}_{n}}{\partial t}\right). \tag{22}$$

The term $\partial T_n/\partial t$ is replaced by $(T_{n+1} - T_n)/\Delta t$ to yield the TG expression for the diffusion equation as

$$Pe\left(\frac{T^{\mathrm{d}}_{n+1} - T^{\mathrm{d}}_{n}}{\Delta t}\right) = \nabla^2 T^{\mathrm{d}}_{n} + \frac{\Delta t}{2} \nabla^2 \left(\frac{T^{\mathrm{d}}_{n+1} - T^{\mathrm{d}}_{n}}{\Delta t}\right). \tag{23}$$

The solution procedure developed by Donea *et al.*[3] proceeds as follows. With a solution T_n available, the TG advection equation (20) is solved for T^{a}_{n+1} with $T^{\mathrm{a}}_{n} = T_n$. Then the TG diffusion equation (23) is solved for T^{d}_{n+1} with $T^{\mathrm{d}}_{n} = T^{\mathrm{a}}_{n+1}$. The solution at t_{n+1} is $T_{n+1} = T^{\mathrm{d}}_{n+1}$. To form a single TG expression, equation (20) is inserted into equation (23), consistent with the above procedure. Keeping terms of low order gives equation (13).

APPENDIX II; NOMENCLATURE

h	height of cavity
L	length of cavity
$\mathbf{n}$	outward-pointing unit vecor for flow boundary
$O(\Delta t)$	terms of order Δt or larger
p	dimensionless isotropic pressure
$\mathbf{q}$	dimensionless heat flux vector
T	dimensionless temperature
T_0, T_1	temperature at $x = 0$ and $x = 4$ (T)
t	dimensionless time
$\mathbf{v}$	dimensionless velocity vector
v_s	characteristic velocity; see equation (7) (L/t)
v_x, v_y	dimensionless x- and y-components of velocity vector
v_x, A	value of v_x at location A; see Figure 1

Greek letters

α	thermal diffusivity (L^2/t)
β	thermal coefficient of volumetric expansion, $-(\partial \ln \rho/\partial T)_p$ (1/T)
γ_v, γ_α	dimensionless coefficients for streamwise diffusion terms; see equations (9) and (10)
$\boldsymbol{\delta}$	unit tensor
δ_k	unit vector in direction k
ε	error specification for time integration
μ	viscosity (M/Lt)
ν	momentum diffusivity (L^2/t)
$\boldsymbol{\pi}$	dimensionless total stress tensor defined in equations (4) and (9)

ρ density (M/L^3)
ψ dimensionless streamfunctions

Superscripts

a solution to thermal advection equation (17)
d solution to thermal diffusion equation (21)
+ dimensional quantity

Subscripts

n index for time step
x, y x- and y-directions

REFERENCES

1. A. N. Brooks and T. J. R. Hughes, 'Streamline upwind/Petrov–Galerkin formulations for convection dominated flows with particular emphasis on the incompressible Navier–Stokes equations', *Comput. Methods Appl. Mech. Eng.*, **32**, 199–259 (1982).
2. J. Donea, 'A Taylor–Galerkin method for convective transport problems', *Int. j. numer. methods eng.*, **20**, 101–119 (1984).
3. J. Donea, S. Giuliani, H. Laval and L. Quartapelle, 'Time-accurate solution of advection–diffusion problems by finite elements', *Comput. Methods App. Mech. Eng.*, **45**, 123–145 (1984).
4. P. M. Gresho, S. T. Chan, R. L. Lee and C. D. Upson, 'A modified finite element method for solving the time-dependent incompressible Navier–Stokes equations. Part 1: Theory', *Int. j. numer. methods fluids*, **4**, 557–598 (1984).
5. M. J. Crochet, F. T. Geyling and J. J. Van Schaftingen, 'Numerical simulation of the horizontal Bridgman growth of a gallium arsenide crystal', *J. Cryst. Growth*, **65**, 166–172 (1983).
6. M. J. Crochet, F. T. Geyling and J. J. Van Schaftingen, 'Numerical simulation of the horizontal Bridgman growth. Part I: Two-dimensional flow', *Int. j. numer. methods fluids*, **7**, 29–47 (1987).
7. K. H. Winters, 'Oscillatory convection in crystal melts: the horizontal Bridgman process', *Proc. 5th Int. Conf. on Numerical Methods in Thermal Problems*, Pineridge, Swansea, 1987, pp. 299–310.
8. B. Roux, G. de Vahl Davis, M. Deville, R. L. Sani and K. H. Winters, 'General synthesis of the results', in B. Roux (ed.), *Numerical Simulation of Oscillatory Convection in Low-Pr Fluids*, Vieweg, Braunschweig, 1990, pp. 285–304.
9. B. Roux and H. Ben Hadid, 'Numerical simulation of oscillatory convection in semiconductor melts', *J. Cryst. Growth*, **97**, 201–216 (1989).
10. M. A. McClelland, 'Time-dependent liquid metal flows with free convection and a deformable free surface', *Int. j. numer. methods fluids*, in press.
11. S. L. Josse and B. A. Finlayson, 'Reflections on the numerical viscoelastic flow problem', *J. Non-Newtonian Fluid Mech.*, **16**, 13–36 (1984).
12. P. Hood, 'Frontal solution program for unsymmetric matrices', *Int. j. numer. methods eng.*, **10**, 379–399 (1976).